ABSOLUTE AND RELATIVE FRENET-SERRET FRAMES FOR ACCELERATED BLACK HOLE CIRCULAR ORBITS [Beating a Dead Horse or Advancing the Cause of Better Understanding Relativistic Kinematics?]

D. BINI
Istituto per Applicazioni della Matematica, C.N.R. , I–80131 Napoli, Italy
and I.C.R.A., Università di Roma, I–00185 Roma, Italy.
e-mail: binid@icra.it

R. T. JANTZEN
Dept.of Math. Sciences, Villanova University, Villanova, PA 19085, USA
and I.C.R.A., Università di Roma, I–00185 Roma, Italy.
e-mail: rjantzen@email.vill.edu

A. MERLONI
I.C.R.A., Università di Roma, I–00185 Roma, Italy.
e-mail: merloni@icra.it

The Frenet-Serret approach is applied in several ways to a familiar but still not geometrically well understood example: circular orbits in black hole spacetimes. An invariant spacetime Frenet-Serret frame approach is useful in understanding the properties of these orbits and of Fermi-Walker transport along them, and provides a visual interpretation of the geometry of this family of orbits. Closely related to the spacetime frame for these special curves are the relative Frenet-Serret frames that may be defined with respect to a family of test observers on the spacetime. The latter connect more directly to our 3-dimensional intuition about the tangent, normal, and binormal to a curve in ordinary space. These absolute and relative frames together help interpret the effects of space curvature, and the gravitoelectric and gravitomagnetic effects on circular orbiting test particles and on their gyroscopic frames of reference.

1 Introduction

The geodesics of a black hole spacetime have been "known" for quite some time thanks to their complete integrability in terms of the four constants of the motion which exist due to the special symmetry of this class of spacetimes. However, "knowing" them and understanding what they tell us about the gravitational field of a black hole are two different things. Effective potentials provide a good tool for appreciating the qualitative behavior of the geodesics, but they don't tell us how the various parts of the gravitational field contribute to that behavior. In fact, our intuition about the kinematics of particle motion is rooted in our 3-dimensional world view, and indeed gravitoelectromagnetic terminology has naturally appeared to characterize an observer-based description of the gravitational field in many applications of general relativity, whether it be in investigating approximate solutions in linearized theory or in studying exact solutions with high symmetry. We relate to forces, and forces tell us how to interpret classical force fields.

It is therefore not a useless exercise to explore test particle motion in important known spacetimes like those describing black holes in order to bridge the gap between the Newtonian picture and the general relativistic one of how the gravi-

tational field "works" in this context. Accelerated circular orbits are a nice case to study because of their high symmetry, because so many distinct families of such orbits characterize important aspects of the geometry of these spacetimes, and because we carry so much baggage about such orbits from Newtonian mechanics which needs to be sorted out in the relativistic regime. Examples are important in any theory in giving us mental pictures of how and why things happen the way they do. Since our mental pictures associated with circular orbits are still a bit cloudy, it is worthwhile devoting some effort to clearing up the situation a bit, even though the literature already has many discussions of this topic (for a review see [1]).

In fact our mental image of a black hole depends on which family of circular orbits we choose to think of as "fixed in space." However, the usual static observers associated with the Boyer-Lindquist coordinate system at the heart of that image of an unchanging space geometry break down near the hole, while the usual ADM geometry associated with the zero-angular momentum observers which remain valid up to the horizon is referred to a family which we think of as being forcibly "dragged around the hole" relative to the static observers, and their geometry is distinct from the geometry of the static space of our mental image. Other circular orbits capture other features of our Newtonian intuition about points fixed in space around a gravitating object, and the acceleration of these various families tells us something about the geometry of spacetime in ways that we can relate to that Newtonian intuition.

The ultimate goal is to add clarity, not just muddy the waters with more formalism, so the present discussion must also place other work into perspective at the same time that it introduces new baggage, or it will be hard to justify. Hence the subtitle of this article.

2 General Frenet-Serret remarks

In classical differential geometry, given an arclength parametrized curve on a Riemannian 3-manifold, one can introduce the unit tangent, normal and binormal in a natural way, providing an orthonormal frame (the Frenet-Serret frame) with which to analyse the geometry of the curve independent of the parametrization as well as important aspects of parametrization-dependent effects. The special case of Euclidean 3-space is a fundamental example in elementary nonrelativistic mechanics, underpinning the concepts of longitudinal and transverse (centripetal) acceleration which still remain almost universal examples in calculus pedagogy. The curvature and torsion scalars characterize the geometry of the curve by giving an equivalent ("osculating") circle of best fit to the curve (or equivalently the angular velocity of the rotating tangent direction within this plane) and the angular velocity (with respect to the arc length parametrization) of the orientation of the plane containing that circle. These in turn help us interpret the components of the acceleration of the time-parametrized curve of a point particle in mechanics along (longitudinal) and perpendicular (transverse) to the direction of motion in terms of the time rate of change of speed and the centripetal acceleration due to the angular velocity about the center of the osculating circle.

One can generalize this procedure to a Riemanian or pseudo-Riemannian man-

ifold any dimension, with one curvature scalar and multiple torsion scalars which together characterize the angular velocity or pseudo-angular velocity of the Frenet-Serret frame compared to one which is parallel transported along the given curve. For the case of spacetime, a Lorentzian 4-manifold, there are two torsions, but the geometry of the Frenet-Serret frame depends on the causal character of the curve: timelike, null, or spacelike. For a spacelike curve with a spacelike "first normal," the situation is similar to the Riemannian case with the curvature (and normal together) describing a circle of best fit to the curve in that spacelike plane (or equivalently the angular velocity of the rotating tangent direction within that plane), and the two torsions determine the rotation of the Frenet-Serret frame in a remaining spacelike plane and a boost of the frame in a single timelike plane formed by pairs of its member vectors. Such curves arise in analysing the time synchronization defect along a closed curve, which exists for a family of observers in spacetime with nonzero vorticity, for example.

However, by far the most interesting curves are the timelike and null curves which represent the motion of nonzero and zero rest mass test particles respectively. Here the timelike case will be considered, where the unit tangent vector is interpreted as the particle 4-velocity and the first normal is the (signed) direction of the acceleration. The curvature, which is the (signed) magnitude of the 4-acceleration, and the first normal then together describe a pseudo-circle (hyperbola) of best fit to the curve or equivalently a pseudo-angular velocity of the boost of the 4-velocity (boost rapidity derivative) compared to one which is parallel transported along the curve. The two torsions then determine the Fermi-Walker angular velocity of the spatial triad of the Frenet-Serret frame, namely its angular velocity compared to a triad which is orthogonal to the tangent vector and Fermi-Walker transported along the curve.

In a spacetime with a preferred family of observers with 4-velocity field u, one can also introduce a space-plus-time "relative" Frenet-Serret frame approach which reconnects with our Euclidean 3-space example so useful in nonrelativistic mechanics. The unit relative velocity of a spacetime curve then plays the role of the tangent, but the normal and binormal in this relative approach depend on the choice of the relative spatial derivative in the local rest space of the observer family where these spatial vectors live, and there are three "natural" choices. This leads to three possible relative centripetal acceleration vectors, for example.

However, one can also introduce a "comoving" relative Frenet-Serret frame along a timelike curve (world line of a nonzero rest mass test particle) adapted to its own local rest space by taking the unit relative velocity of the curve with respect to the observer family within that rest space as the first Frenet-Serret vector, its natural unique Fermi-Walker derivative along the curve as the normal, and their spatial cross-product as the bi-normal. This models the test particle's reconstruction of its relative motion as seen by the observer family, and corresponds in some sense to our notion of how one would see one's own motion in the "space" of the black hole spacetime. These relative frames are discussed in the companion article[2,3] in these proceedings.

3 General gyro spin remarks

The precession of the spin of a gyroscope in a gravitational field is an exciting consequence of relativistic gravitational theory compared to the Newtonian case, but since test gyros actually define what it means for a direction to be "nonrotating," their precession only makes sense as a relative effect. For a generic spacetime it is problematic to decide what to compare the spin direction to locally, but in stationary axisymmetric spacetimes, the symmetry provides a rigid connection to nonrotating observers at infinity through the usual static observers following the Killing vector trajectories which are the Boyer-Lindquist time coordinate lines.

For observers at the same spacetime point but in relative motion, the orientation of a set of orthonormal spatial axes carried by the other observer is understood to be the orientation of the axes which are boosted back to the observer doing the observing. This assumption is inherent in the diagrams of primed and unprimed 3-frames in relative motion when we discuss inertial frames in elementary special relativity. All observers in a stationary axisymmetric spacetime in circular motion therefore agree on the orientation of any particular set of axes at a given spacetime point since their relative velocities are all "collinear" and the family of boosts along a fixed direction forms a group. (If three observers were not collinear, i.e., had linearly independent 4-velocities, boosting one's orthonormal frame to the local rest spaces of the other two, and then boosting either one of the latter to the other's local rest space would yield a frame differing by a rotation from the one boosted directly back to that local rest space from the original observer.) The precession rate of a set of gyro fixed axes along a given world line with respect to a fixed parametrization of the world line and a fixed set of reference axes is therefore observer-independent in this class of observers. (Observer proper time parametrizations then lead to differing rates.) The normalized Boyer-Lindquist spatial coordinate frame (boosted to the world line local rest space) provides a natural set of reference axes for circular motion. Since these frames rotate along a circular orbit with respect to nonrotating frames at spatial infinity with the orbital angular velocity, a subtraction must be performed to remove this additional rotation.

However, the question of the total precession during one revolution of a circular orbit does depend on which observer family the revolution is taken with respect to, since completion of a revolution is marked by the return to the original observer whose path is crossed at its start. Usually the static observers are used to mark revolutions with respect to nonrotating observers at spacelike infinity, although this only works outside the ergosphere of a black hole.

4 Circular orbits and Frenet-Serret formalism

The spacetime Frenet-Serret frame along the single timelike test particle world line with 4-velocity $U = e_0$, parametrized by the proper time τ, is described by the equations[5,6]

$$\frac{\mathrm{D}}{\mathrm{d}\tau} e_0 = \kappa\, e_1 \ , \qquad\qquad \frac{\mathrm{D}}{\mathrm{d}\tau} e_2 = -\tau_1 e_1 + \tau_2 e_3 \ ,$$

$$\frac{\mathrm{D}}{\mathrm{d}\tau}e_1 = \kappa\, e_0 + \tau_1\, e_2 \ , \quad \frac{\mathrm{D}}{\mathrm{d}\tau}e_3 = -\tau_2 e_2 \ , \tag{1}$$

namely

$$\mathrm{D}e_\alpha/\mathrm{d}\tau = L^\beta{}_\alpha\, e_\beta \ , \tag{2}$$

where the matrix $(L^\alpha{}_\beta)$ belongs to the Lie algebra of the Lorentz group. The curvature κ is allowed to be of either sign in order that the frame may be extended smoothly through isolated points where $\mathrm{D}U/\mathrm{d}\tau = 0$. Its absolute value is the magnitude of the acceleration $a = \kappa e_1$ and describes the rate of change of the rapidity parameter of the boost of the Frenet-Serret frame relative to an orthonormal frame parallel transported along the world line.

The first and second torsions τ_1 and τ_2 are the components of the Frenet-Serret angular velocity vector

$$\omega_{(\mathrm{FS})} = \tau_2 e_1 + \tau_1 e_3 \tag{3}$$

of the spatial frame $\{e_a\}$ with respect to one Fermi-Walker transported along the curve,[4] i.e.,

$$\mathrm{D}_{(\mathrm{fw})}e_a/\mathrm{d}\tau = \omega^c_{(\mathrm{FS})a}\, e_c = \epsilon_{bca}\omega^b_{(\mathrm{FS})}e_c \ , \tag{4}$$

where $\mathrm{D}_{(\mathrm{fw})}/\mathrm{d}\tau$ is the projection orthogonal to U of the intrinsic derivative, namely the spatial Fermi-Walker derivative. The sign-reversed angular velocity $-\omega_{(\mathrm{FS})}$ therefore describes the precession angular velocity with respect to the Frenet-Serret frame of the Fermi-Walker transported spin vector of a test gyroscope moving along the world line of U.[4]

Consider the Boyer-Lindquist line element for the Kerr spacetime orthogonalized with respect to $n = N^{-1}(\partial_t - N^\phi\partial_\phi)$ (the unit normal to the Boyer-Lindquist time slicing of the Kerr spacetime and the 4-velocity of zero angular momentum observers or ZAMO's), leading to the lapse-shift form

$$\mathrm{d}s^2 = -N^2\mathrm{d}t^2 + g_{\phi\phi}(\mathrm{d}\phi + N^\phi\mathrm{d}t)^2 + g_{rr}\mathrm{d}r^2 + g_{\theta\theta}\mathrm{d}\theta^2 \ . \tag{5}$$

The mutually orthogonal (t,ϕ) and (r,θ) subspaces of the tangent space reflect the $2+2$ splitting associated with the orthogonal transitivity symmetry of the spacetime. Most of the present remarks also apply to the wider class of orthogonally transitive stationary axisymmetric spacetimes. For definiteness, it is assumed that the black hole angular momentum parameter a satisfies $a \geq 0$ so that the black hole is rotating in the positive ϕ direction when $a \neq 0$. The context should always clearly distinguish the symbol a for the acceleration used below from the traditional angular momentum parameter a of the Kerr metric. The dimensionless parameter $\bar{a} = a/\mathcal{M}$ and radial variable $\bar{r} = r/\mathcal{M}$ are also useful, where $\mathcal{M}$ is the black hole mass parameter.

Furthermore, stationary axisymmetric quantities depend only on (r,θ), which are simplest to visualize by representing them graphically in the ρ-z coordinate plane of the corresponding flat spacetime cylindrical coordinates $(\rho, z) = (r\sin\theta, r\cos\theta)$; the $\pm\rho$ coordinate directions will be referred to as "horizontally outward" and "horizontally inward" respectively away from and towards the "vertical" symmetry axis $\rho = 0$. Similarly the z coordinate direction will be referred to as "vertical," either away from or towards the equatorial plane $z = 0$ or $\theta = \pi/2$.

World lines which correspond to circular orbits with constant speed $|\nu|$ (with respect to the ZAMO's) have 4-velocity

$$e_0 = U = \Gamma(\partial_t + \zeta\partial_\phi) = \gamma(n + \nu\partial_{\hat{\phi}}) = \cosh\alpha\, n + \sinh\alpha\, \partial_{\hat{\phi}} \ , \tag{6}$$

where the relative velocity $\nu\partial_{\hat{\phi}}$ has constant signed magnitude $\nu = \tanh\alpha \in (-1, 1)$ parametrized by the rapidity $\alpha \in (-\infty, \infty)$, in terms of which the following useful relations hold

$$[\gamma, \gamma\nu, \nu, \gamma^2(1+\nu^2), 2\gamma^2\nu] = [\cosh\alpha, \sinh\alpha, \tanh\alpha, \cosh 2\alpha, \sinh 2\alpha] \ . \tag{7}$$

The rapidity is the natural pseudo-angular parameter for the hyperbola of such 4-velocities in the (t, ϕ) subspace of the tangent space, the relative observer plane for the set of all such observers at each spacetime point, and for more simply expressing certain naturally occurring functions of the relative velocity. Circular orbits with $\nu > 0$ (positive angular momentum) will be referred to as co-revolving, while those with $\nu < 0$ (negative angular momentum) will be referred to as counter-revolving, following the terminology of Wilkins.[7]

The acceleration of these orbits $a = \mathrm{D}U/\mathrm{d}\tau$ may be parametrized by polar coordinates in the $\partial_{\hat{r}}$-$\partial_{\hat{\theta}}$ plane in the tangent space to which they are confined (the "acceleration plane"), namely the signed magnitude κ of the acceleration and its orientation angle χ, both of which are constants along a given orbit and in turn functions of the rapidity α parametrizing all such orbits

$$a = \kappa(\cos\chi\, \partial_{\hat{r}} + \sin\chi\, \partial_{\hat{\theta}}) \ , \qquad |\kappa| = [(a^{\hat{\theta}})^2 + (a^{\hat{r}})^2]^{1/2} \ , \ \tan\chi = a^{\hat{\theta}}/a^{\hat{r}} \ . \tag{8}$$

If we choose the convention $\kappa \geq 0$, $\chi \in [-\pi, \pi]$, the direction of the acceleration is

$$e_1 = \cos\chi\, \partial_{\hat{r}} + \sin\chi\, \partial_{\hat{\theta}} \ . \tag{9}$$

Since e_1 and U are 1-parameter families of unit vectors, their angular/pseudo-angular derivatives must be orthogonal to them. In fact the final pair of Frenet-Serret vectors are

$$\begin{aligned} e_2 &= \mathrm{d}U/\mathrm{d}\alpha = \sinh\alpha\, n + \cosh\alpha\, \partial_{\hat{\phi}} \ , \\ e_3 &= -\mathrm{d}e_1/\mathrm{d}\chi = \sin\chi\, \partial_{\hat{r}} - \cos\chi\, \partial_{\hat{\theta}} \ , \end{aligned} \tag{10}$$

the latter vector being the clockwise rotation of e_1 by 90 degrees in the ∂_r-∂_θ plane, making the triad $\{e_a\}$ righthanded. Thus the e_0-e_2 relative velocity plane and the orthogonal e_1-e_3 acceleration plane (transverse to all such velocities, characterizing purely transverse relative acceleration for any observer of the same type) reflect the $2 + 2$ orthogonal transitivity splitting.

The outward (+) and inward (−) (with respect to the symmetry axis) "horizontal" directions along $\pm\partial_{\hat{\rho}}$ in the $\partial_{\hat{r}}$-$\partial_{\hat{\theta}}$ plane correspond to the values $\chi_\pm = \pm\pi/2 - \theta$, while $\chi \in (-\pi/2, \pi/2)$ corresponds to outward acceleration $a^{\hat{r}} > 0$ with respect to the radial direction, and the complementary half-plane to inward such acceleration. Our convention that $\kappa \geq 0$ means that as $r \to \infty$, then $\chi \approx \chi_-$ for sufficiently large ν in region A, i.e., the acceleration is horizontally inward toward the symmetry axis

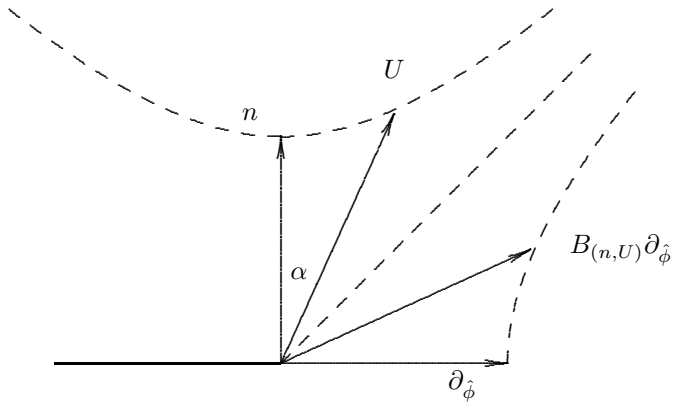

Figure 1: The hyperbola of unit 4-velocities U of the timelike circular orbits in the relative observer plane for circular motion, spanned by the orthogonal vectors n and $\partial_{\hat{\phi}}$. Spacelike circular orbits have unit tangents which are related by a boost to $\partial_{\hat{\phi}}$.

far from the black hole at a high enough speed, corresponding to the flat spacetime inward centripetal acceleration along $-\partial_{\hat{\rho}}$. As one approaches the black hole above the equatorial plane, the ultrarelativistic acceleration vectors tilt farther up, rotating away from the symmetry axis towards the outward radial direction to resist the increasingly strong attraction toward the hole.

Our mental picture of a black hole corresponds to the projected spatial coordinate geometry on the (r, θ, ϕ) coordinate space which parametrizes the space of static (Killing) observers following the time coordinate lines with 4-velocity $m = \partial_{\hat{t}}$, a geometry which differs from the induced spatial coordinate geometry characterizing the space of the ZAMO observers. In the corresponding flat spatial geometry of our Newtonian picture on this same space, $-\partial_\rho$ is the normal to the spatial curve having unit tangent along the ϕ coordinate direction, while the binormal is along the z coordinate direction. These also correspond to the relative Frenet-Serret frame vectors, but differ by relativistic effects.[3]

As α varies from $-\infty$ to ∞, or ν from -1 to 1, the 4-velocity U traces out one branch of a hyperbola (pseudocircle) in the relative observer plane, while the acceleration vector a traces out one branch of a hyperbola (to be shown below) in the orthogonal transverse relative acceleration plane whose properties depend on the location of the tangent space, i.e., on r and θ.

The second branch of this hyperbola corresponds to superluminal motion (a spacelike circular orbit) with $\nu^{-1} \in (-1, 1)$, which includes the closed ϕ-coordinate circles. Figures 1 and 2 illustrate these curves.

The line element in the acceleration plane

$$\mathrm{d}s_{(\mathrm{a})}{}^2 = \mathrm{d}\kappa^2 + \kappa^2 \mathrm{d}\chi^2 \tag{11}$$

measures the arclength along this curve of acceleration vectors in the tangent space. With the above choices for e_1 and e_3, the two torsions must be allowed to change sign. They are then simply equal to half the sign-reversed rate of change of the

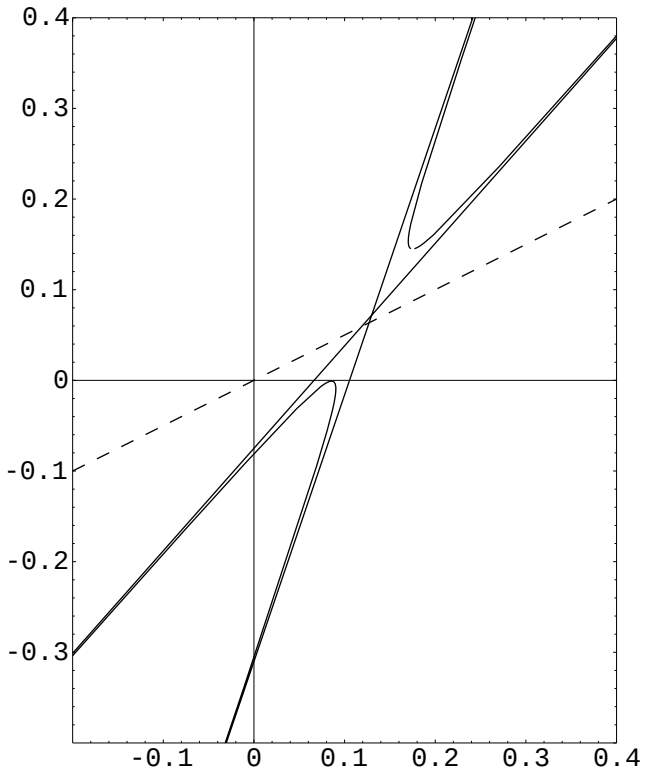

Figure 2: The hyperbola of acceleration vectors of the nonnull circular orbits in the acceleration plane for circular motion, spanned by $\partial_{\hat{r}}$ (horizontal axis) and $\partial_{\hat{\theta}}$ (vertical axis), shown for $\bar{a} = 0.5$, $\theta = \pi/3$, $\bar{r} = 4$. The dashed line is along the "horizontal" direction, with $\partial_{\hat{\rho}}$ pointing to the left along it towards the symmetry axis. The lower branch represents the timelike orbits whose right half corresponds to the counter-rotating orbits whose acceleration vectors must have a larger (outward) radial component to resist the greater attraction to the black hole. The upper branch represents the spacelike orbits, with the closed ϕ coordinate circle near its vertex.

arclength along the two polar coordinate directions with respect to α

$$\tau_1 = -\frac{1}{2}\mathrm{d}\kappa/\mathrm{d}\alpha \ , \quad \tau_2 = -\frac{1}{2}\kappa \mathrm{d}\chi/\mathrm{d}\alpha \ . \tag{12}$$

The tangent to the acceleration hyperbola and consequently the Frenet-Serret angular velocity (3) can therefore be expressed as

$$\frac{\mathrm{d}a}{\mathrm{d}\alpha} = \frac{\mathrm{d}\kappa}{\mathrm{d}\alpha}e_1 + \kappa\frac{\mathrm{d}e_1}{\mathrm{d}\alpha} = 2(-\tau_1 e_1 + \tau_2 e_3) \ , \qquad \omega_{(\mathrm{FS})} = \frac{1}{2}e_2 \times_U \frac{da}{d\alpha} \ . \tag{13}$$

Thus $\omega_{(\mathrm{FS})}$ is obtained from $\frac{1}{2}\mathrm{d}a/\mathrm{d}\alpha$ by a counterclockwise rotation of 90 degrees with respect to the ordered axes (e_3, e_1), which have the same orientation as $(\partial_{\hat{r}}, \partial_{\hat{\theta}})$, placing it along the inward normal to the hyperbola as will be seen below. Its magnitude

$$||\omega_{(\mathrm{FS})}|| = (\tau_1^2 + \tau_2^2)^{1/2} = \frac{1}{2}\left[(\mathrm{d}\kappa/\mathrm{d}\alpha)^2 + \kappa^2\left(\mathrm{d}\chi/\mathrm{d}\alpha\right)^2\right]^{1/2} = \frac{1}{2}\left|\mathrm{d}s_{(\mathrm{a})}/\mathrm{d}\alpha\right| \tag{14}$$

is just half the speed with which the acceleration curve is traced out in its plane with respect to the α parametrization. The Frenet-Serret angular velocity traces out a curve in the acceleration plane which is also a hyperbola with its asymptotes rotated by 90° but lying in a complementary branch (the opening angles of the two hyperbolas sum to π). The derivation of these simple torsion formulas (12) on which all of this beautiful geometry rests starts from eqs. (49), (54) of Iyer and Vishveshwara.[4] They apply to the entire orthogonally transitive stationary axisymmetric symmetry class of spacetimes, enabling one to convert their lengthy formulas into concrete geometry nicely illustrated by 2-dimensional graphics.

5 Geometry of the transverse relative acceleration plane

The orthonormal components of the parametrized acceleration hyperbola in the $\partial_{\hat{r}}$-$\partial_{\hat{\theta}}$ plane have the fractional quadratic form

$$a^{\hat{r}} = \mathcal{F}(\nu; k^{\hat{r}}, \nu_+^{(r)}, \nu_-^{(r)}) \ , \ a^{\hat{\theta}} = \mathcal{F}(\nu; k^{\hat{\theta}}, \nu_+^{(\theta)}, \nu_-^{(\theta)}) \ , \tag{15}$$

where $\nu = \tanh\alpha \in (-1,1)$ and (using Eq. (7))

$$\begin{aligned}\mathcal{F}(\nu; k, \nu_+, \nu_-) &= k\frac{(\nu-\nu_-)(\nu-\nu_+)}{1-\nu^2} \\ &= k[\sinh^2\alpha - (\nu_- + \nu_+)\sinh\alpha\cosh\alpha + \nu_-\nu_+\cosh^2\alpha] \\ &= \frac{1}{2}k[(\nu_-\nu_+ + 1)\cosh 2\alpha - (\nu_- + \nu_+)\sinh 2\alpha + (\nu_-\nu_+ - 1)] \ . \end{aligned} \tag{16}$$

Thus with the natural rapidity parametrization, the acceleration curve takes the matrix form

$$\begin{bmatrix} a^{\hat{r}} \\ a^{\hat{\theta}} \end{bmatrix} = \begin{bmatrix} A & B \\ C & D \end{bmatrix} \begin{bmatrix} \cosh 2\alpha \\ \sinh 2\alpha \end{bmatrix} + \begin{bmatrix} E \\ F \end{bmatrix} \ . \tag{17}$$

Solving this for $\cosh 2\alpha, \sinh 2\alpha$ and using the identity $\cosh^2 2\alpha - \sinh^2 2\alpha = 1$, one immediately finds the explicit form for the unparametrized equation of a general hyperbola with center $[E, F]$ displaced from the origin

$$\begin{bmatrix} a^{\hat{r}} - E & a^{\hat{\theta}} - F \end{bmatrix} \begin{bmatrix} A & B \\ C & D \end{bmatrix}^{-1\,\mathrm{T}} \begin{bmatrix} 1 & 0 \\ 0 & -1 \end{bmatrix} \begin{bmatrix} A & B \\ C & D \end{bmatrix}^{-1} \begin{bmatrix} a^{\hat{r}} - E \\ a^{\hat{\theta}} - F \end{bmatrix} = 1 \ . \tag{18}$$

A change of observer corresponds to a translation in α which in turn leads to an $SL(2,R)$ transformation of the matrix of coefficients.

The Frenet-Serret angular velocity vector $\omega_{(\mathrm{FS})}$ is obtained from the acceleration vector by half the α-derivative, which interchanges $\cosh 2\alpha$ and $\sinh 2\alpha$, and a counterclockwise rotation by $\pi/2$

$$\begin{bmatrix} \omega^{\hat{r}}_{(\mathrm{FS})} \\ \omega^{\hat{\theta}}_{(\mathrm{FS})} \end{bmatrix} = \begin{bmatrix} 0 & -1 \\ 1 & 0 \end{bmatrix} \begin{bmatrix} A & B \\ C & D \end{bmatrix} \begin{bmatrix} 0 & 1 \\ 1 & 0 \end{bmatrix} \begin{bmatrix} \cosh 2\alpha \\ \sinh 2\alpha \end{bmatrix} \ . \tag{19}$$

This is a hyperbola centered at the origin with complementary asymptotes to the acceleration hyperbola rotated by 90 degrees. The minimum value of the magnitude

$||\omega_{(\mathrm{FS})}||$ clearly occurs at its vertex, which corresponds to the same relative velocity $\nu_{(\mathrm{vert})} = \tanh \alpha_{(\mathrm{vert})}$ describing the vertex of the acceleration hyperbola, defining a family of "extreme Fermi-Walker rotation" observers.

These general properties characterize the timelike circular orbits in any orthogonally transitive stationary axisymmetric spacetime. For the Kerr spacetime, one may use a computer algebra system to study the particular functions of r and θ which determine the behavior of the acceleration and Frenet-Serret hyperbolae as a function of position in order to give some insight into how the behavior differs from the Newtonian case. This has been done and discussed in detail in reference [8], so a complimentary discussion of their qualitative behavior will be given here.

The key difference with the picture of the static Newtonian gravitational field of an isolated stationary axially symmetric rotating source is that the natural (unaccelerated) stationary observers "at rest in space" in the Newtonian case correspond to the accelerated "static" observers in the relativistic case (those following the time coordinate lines in the Boyer-Lindquist coordinate system, along Killing trajectories, said to be nonrotating with respect to spatial infinity), so the acceleration vectors in the two cases differ by the acceleration needed to remain fixed in "space," which is itself an ambiguous concept in the relativistic regime. Thus the 4-acceleration of a circular orbit consists of the sum of a relative centripetal acceleration associated with the circular motion with respect to the observer family together with the acceleration needed by the observer family to resist the gravitational attraction, two pieces which individually remain ambiguous since there are a number of choices for the decomposition.

Furthermore, it is the locally nonrotating observers or ZAMO's which prove more useful than the static observers since the ZAMO's remain well defined right up to the horizon of a black hole spacetime, while the static observers are unable to remain "fixed in space" within the ergosphere. On the other hand the ZAMO's are "dragged around" the hole compared to the static observers, and while the "infinitesimal connecting vector" between nearby ZAMO's does not rotate with respect to Fermi-Walker propagated axes along their world lines because their vorticity vanishes, their acceleration vector does rotate with respect to such axes in the Kerr case. Since static observers follow Killing trajectories, their acceleration vector and nearby observers are locked together undergoing a rotation compared to Fermi-Walker propagated axes with an associated angular velocity which is the vorticity vector modulo sign.[4]

However, in the nonrotating Schwarzschild case, these two observer families coincide and also exhibit another feature of the Newtonian case: their 4-acceleration is extremal. In the Newtonian case, the circular orbiting observers at rest in space have the maximum radial acceleration, namely zero, compared to the negative (radially inward) radial acceleration for all objects in circular motion, due to their inward centripetal acceleration in the direction of the axis of symmetry. This is a minimum of the magnitude of the acceleration. In the relativistic nonrotating case this behavior of the relative centripetal acceleration is superimposed on the acceleration needed to resist the gravitational acceleration of the hole, but it is still a maximum of the radial component at least far enough from the hole, as well as a local maximum of the magnitude of the total 4-acceleration. In the rotating case,

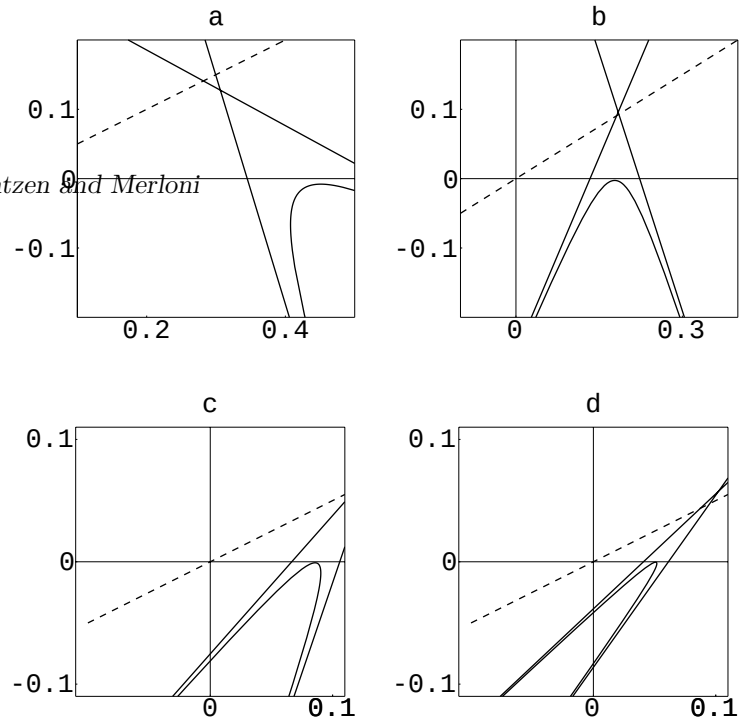

Figure 3: The acceleration hyperbolae in the tangent space (horizontal axis along $\partial_{\hat{r}}$, vertical axis along $\partial_{\hat{\theta}}$) for regions A, B, and C for $\bar{a} = 0.5$, shown at a typical angle $\theta = \pi/3$ at radii (a) $\bar{r} = 2.25$ (region C), (b) $\bar{r} = 3$ (region B), (c) $\bar{r} = 4$ (region A), (d) $\bar{r} = 5$ (region A). The dashed line represents the "horizontal" direction in the ρ-z plane, with the symmetry axis to the left along it at the polar angle $\chi_- = -5\pi/6$, and the equatorial plane above it. Figure 9 shows the orientation of these diagrams in the ρ-z plane for the same angle. The hyperbola rotates inward as r increases (counterclockwise in this figure) and centripetal acceleration becomes more dominant, finally reaching a configuration like (d) where 3 local extrema of κ (the distance from the origin) are obvious.

these "extremely accelerated observers"[10–12] are yet a third family, characterized by an extreme value of the magnitude of the total 4-acceleration (one of 3 distinct extremal values which exist for most radii), which in turn differs from the extreme value of the radial component.[13] This is typical of the way in which concepts which are unambiguous in the nonrelativistic case have multiple generalizations in the relativistic case, where properties which hold simultaneously in the nonrelativistic context no longer do so.

Figure 3 shows how the acceleration hyperbola above the equatorial plane at a fixed angle $\theta = \pi/3$ rotates upward (from the inward horizontal direction far from the hole) and outward (towards the outward radial direction) as one approaches the hole from far away, while the vertex of the hyperbola moves farther out in the radial direction, as more and more radially outward acceleration is needed to oppose the increasingly stronger nearly radial gravitational attraction towards the hole. Simultaneously the asymptotes of the hyperbola open up as the increasingly stronger dragging effect increasingly separates the acceleration directions of ultrarelativistic corevolving and counter-revolving orbits until a maximum opening angle is reached very near the hole beyond which they instead squeeze closer and closer together and to the outward radial direction, with the opening angle going to zero at the horizon. The directions of the two asymptotes themselves are the directions of the acceleration vectors of the counter and corotating photon orbits. The asymptote which is to the right (rotated further towards the outward radial direction) in figure

3 corresponds to $\nu \to -1$ (the counter-rotating photon), while the one to the left corresponds to $\nu \to 1$ (the corotating photon), which reflects the fact that counter-revolving (corevolving) orbits require a stronger (weaker) radial acceleration to resist the increased (decreased) gravitational attraction due to the contribution from the gravitomagnetic force, in the relative observer description of reference [14] (see figure 2 there). The next section will analyze the contributions of the various aspects of the spacetime geometry (space curvature, gravitoelectric and gravitomagnetic effects) to the behavior of the acceleration hyperbola, using the relative observer decomposition of the acceleration.

Figure 3 also reveals the geometry of the extremal acceleration points of the acceleration hyperbola[10–12] as a function of the radius, which occur when the position vector of the point on the hyperbola is orthogonal to its tangent vector (and therefore aligned with the Fermi-Walker angular velocity modulo sign), since the distance from the origin in the acceleration plane is the magnitude of the acceleration being extremized. Far from the hole as in figure 3(a), there is one global minimum on the origin side of the hyperbola and two local extrema, one maximum and one minimum, on the far side. As one approaches the hole (figures 3(b) and 3(c)), the symmetry axis of the hyperbola rotates towards the outward radial direction until these two local extrema coalesce and then disappear, leaving only the global minimum behind.

At each radius for fixed angle θ there is also a single global minimum $|\chi_{(\min)}|$ of the absolute value of the acceleration angle, where the position vector is tangent to the hyperbola (and therefore orthogonal to the Fermi-Walker rotation), near its vertex. This angle is the minimum acute angle that the acceleration vector is tilted upward (downward) from the radial direction above (below) the equatorial plane. Examining this extreme value as a function of the radius for fixed angles, it turns out to be extremely small with a sharp peak near the black hole with a maximum value less than roughly .0025 (about .15 degrees) even for an extreme black hole. As the horizon is approached, even the photons are unable to resist the increasing radial attraction of the hole so the radial acceleration component overwhelms the tangential one for both corotating and counter-rotating photons, and the acceleration hyperbola branch squeezes to the outward radial direction, taking this angle back to zero. The relative velocity $\nu^{(\chi)} < 0$ at which the extreme value of ξ occurs is very small as is the relative velocity $\nu^{(\theta)} > 0$ at which $|a_{\hat{\theta}}|$ is minimized (horizontal tangent to the acceleration curve), both of which are sharply peaked at the same radius for a given θ very close to the hole with a maximum on the order of 10^{-3}. Thus the ZAMO's lie somewhere between the horizontal tangent and the point of tangency of the position vector on the acceleration hyperbola.

The orientation of the acceleration hyperbola can be characterized by whether the two photon acceleration asymptotes have a positive or negative radial component, i.e., are tilted radially outward or inward compared to the tangential θ direction. Far from the hole they are both initially tilted inward (region A), but first the counter-rotating photon acceleration rotates to an outward tilt (region B), and is then joined by the corotating photon acceleration in tilting outward (region C) near the hole, as illustrated respectively in figures 3(a), 3(b), and 3(c). Because of the orientation of the hyperbola in the acceleration plane, this is correlated with

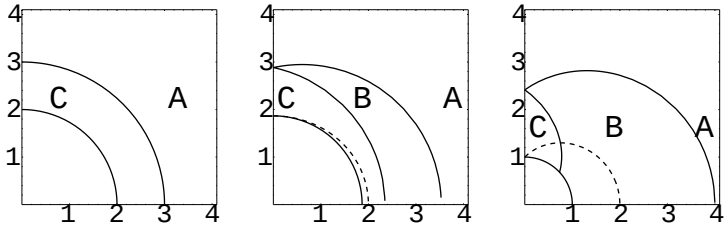

Figure 4: The profiles of the regions A, B, and C for a black hole with $\bar{a} = 0$ (left), $\bar{a} = 0.5$ (center) and $\bar{a} = 1$ (right) represented in the ρ-z coordinate plane (horizontal axis ρ, vertical axis z), showing the ergosphere boundary (dashed line) and the horizon (innermost curve). In the $\bar{a} = 0$ limit (see figure 3a), region B collapses to the sphere $\bar{r} = 3$, while the ergosphere collapses to the horizon $\bar{r} = 2$. In the $\bar{a} = 1$ limit (see figure 3c), region C collapses to the horizon for angles greater than the angle $\theta_* \simeq 47^0$. Region C continues to exist at smaller angles.

the number of zeros of the radial acceleration (where the hyperbola crosses the $\partial_{\hat{\theta}}$ axis), namely 2 (region A), 1 (region B), and 0 (region C). The two roots $\nu_{\pm}^{(r)}$ of the radial acceleration $a^{\hat{r}}$ are always real and of opposite sign and describe the circular orbits with vanishing radial acceleration, reducing to geodesics in the equatorial plane, where the acceleration is purely radial. Both velocities are subluminal at sufficiently large radius, leading to a pair of orbits with vanishing radial acceleration, but as one approaches the black hole first the counter-revolving velocity $\nu_{-}^{(r)}$ and then also the corevolving velocity $\nu_{+}^{(r)}$ become superluminal, defining three regions A (both subluminal, far from the hole), B (one subluminal, one superluminal), and C (both superluminal, close to the hole) exactly as discussed for the equatorial plane geodesics in reference [9] to which this discussion reduces in the equatorial plane case. In region C, the acceleration is always radially outward ($a^{\hat{r}} > 0$), while in region B the ultrarelativistic counter-revolving acceleration is radially outward but the ultrarelativistic corevolving acceleration is inward.

The interface radii $r_{\rm AB}(\theta)$ and $r_{\rm BC}(\theta)$ separating these three regions occur respectively where the counter-rotating and corotating photon orbits have zero radial acceleration (namely $\nu_{-}^{(r)} = -1$ and $\nu_{+}^{(r)} = 1$) and the corresponding asymptote of the acceleration hyperbola is vertical in the acceleration plane. The middle region B collapses to the sphere $\bar{r} = 3$ in the Schwarzschild limit $\bar{a} = 0$. Figure 4 illustrates these three regions in the ρ-z coordinate plane for $\bar{a} = 0, 0.5, 1$. In the extreme case $\bar{a} = 1$, the curve separating region C and B bifurcates on the horizon, while region B squeezes up against the horizon up until that bifurcation point for $\bar{a} \to 1$. The details are discussed in the appendix.

Figure 5 illustrates the behavior of the acceleration magnitude κ as a function of ν for selected radii in the three regions A, B, C at a typical angle of $\theta = \pi/3$. In most of region A extending out to infinity (lower curves), there are 3 local extrema of κ where the position vector in the 2-plane of the acceleration hyperbola is orthogonal to its tangent line, occurring at the ZAMO relative velocities $\nu_{-1}^{(\kappa)} < \nu_{-2}^{(\kappa)} < 0 < \nu_{+}^{(\kappa)}$ (local min, local max, global min respectively). As one approaches the hole the local max and min coallesce, leaving only a single global minimum near the hole

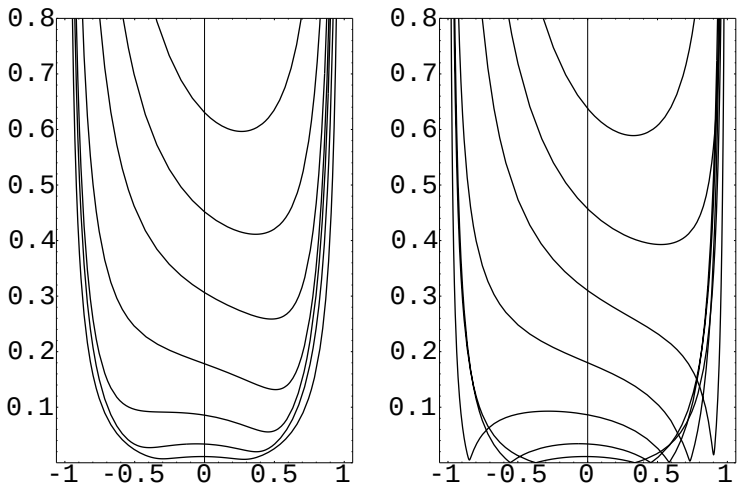

Figure 5: The magnitude κ of the acceleration versus ZAMO relative velocity $\nu \in (-1, 1)$ for selected radii in regions A (lower curves), B (intermediate curves), and C (upper curves) at a typical angle $\theta = \pi/3$ (left) and near the equatorial plane at for $\bar{a} = 0.5$. The close proximity to the circular geodesics ($\kappa = 0$) in that plane is clearly seen at the kinks in the curves near the horizontal axis.

(upper curves).

The angular opening of the pair of asymptotes of the acceleration hyperbola increases with $\bar{a}$ and decreases to zero when $\bar{a} = 0$. Figure 6 shows the limiting case $\bar{a} = 0$ of the Schwarzschild spacetime where the branch of the acceleration hyperbola degenerates to a half line terminating on the axis of purely radial acceleration at $\nu = 0$, traced once for each sign of ν. This half line intersects the zero radial acceleration ($e_{\hat{\theta}}$) axis in a single point in region A but as one moves towards the black hole, this half line rotates away from the symmetry axis towards the outward radial direction, aligning itself parallel to the zero radial acceleration axis ($e_{\hat{\theta}}$) at the interface with region C (region B shrinks to a surface), beyond which it is tilted away from that axis and thus has no intersection. The angle of tilt reveals the competition between the outward radial acceleration necessary to resist falling into the hole and the centripetal acceleration towards the symmetry axis perpendicular to the circular orbit.

In the rotating case, the angular opening of the pair of asymptotes increases from zero far away from the hole to a maximum roughly in regions B and C and then decreases back to zero at the horizon. This is illustrated in figure 7 for selected angles between 0 and $\pi/2$ for $\bar{a} = 0.5$. As the equatorial plane is approached, this angle approaches a step function with value π in region B and zero in regions A and C, reflecting the behavior of the purely radial component of the acceleration there as plotted in figure 6(c) of [9].

Figure 4 of reference [8] illustrates the velocities of the various special circular orbits with respect to the ZAMO's at selected values of θ, generalizing the equatorial plane case shown in figure 7(b) of reference [9]. These include the extremal acceleration observers corresponding to the extremal values of the acceleration magnitude

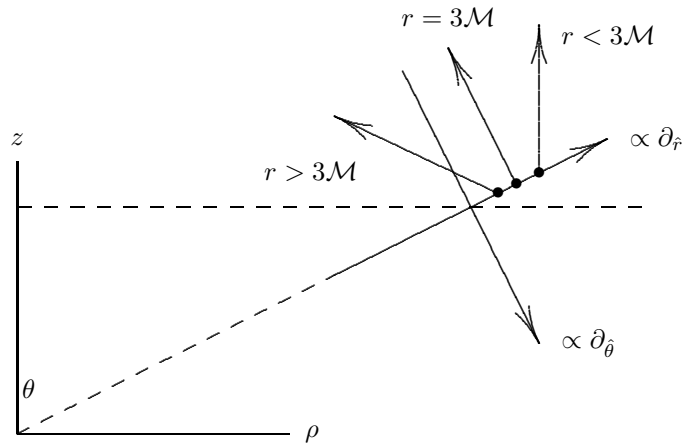

Figure 6: The degenerate acceleration hyperbola half lines for the Schwarzschild case for timelike circular orbits. Their directions are those of the acceleration of the photon orbits.

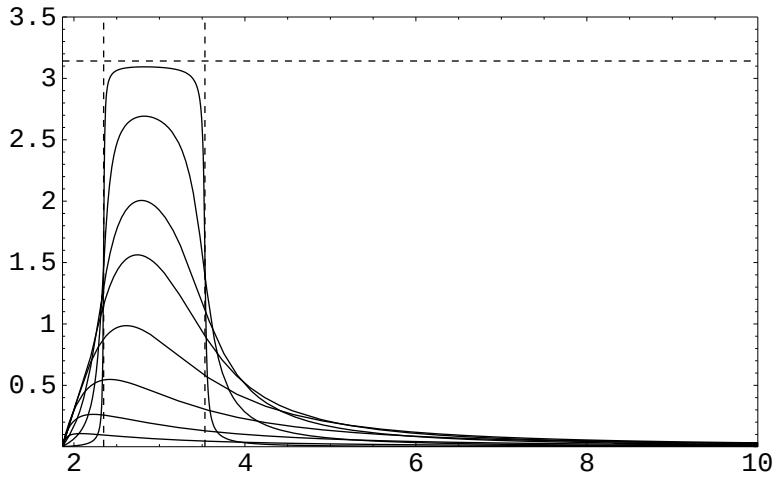

Figure 7: The maximum opening angle in radians for the acceleration hyperbola as a function of $\bar{r}$ outside the horizon for $\bar{a} = 0.5$ and $\theta = \pi/2.1, \pi/2.3, \pi/2.5, \pi/3, \pi/4, \pi/6, \pi/10$ (from top to bottom). The vertical dashed lines denote the equatorial radii of the interfaces between regions A, B, and C.

discussed above.

6 The relative observer decomposition of the acceleration

Given what we all know about Newtonian gravity and the very useful notions of centripetal acceleration / centrifugal force in the description of orbits in such fields, it is worth trying to understand how the picture may be stretched to fit the relativistic case. The gravitational field is sensed through the motion of test particles, and given that our mental picture of a black hole, like the corresponding nonrelativistic gravitational field, is based on an implicit family of test observers, it is only natural to analyze the gravitational field by calculating how these test observer families view test particle motion. This subject has a long and rich history[1] that gave rise to the terminology of "gravitoelectric" and "gravitomagnetic" fields, two of the three aspects of spacetime geometry which result from splitting spacetime into space-plus-time through an observer family decomposition, the remaining one being space curvature. It is also somewhat obscured by a Fermat's theorem approach to light ray paths in stationary spacetimes which leads to a conformal transformation of the spatial geometry used to discuss nonzero rest mass motion. This has its origins in old work by Møller, but has been analyzed geometrically in detail for black hole spacetimes by Abramowicz and many collaborators. While this is a nice geometrization of the relative motion of test particles and light rays in static spacetimes, it seems less useful in more general stationary spacetimes where the gravitomagnetic effect cannot be absorbed into the spatial geometry, and appears to be no longer useful in nonstationary spacetimes. However, it leads to some semantical controversy over claims for the "correct generalization" of centrifugal and Coriolis forces to general relativity. Such debates can of course never be won since the richness of general relativity removes the degeneracy of many properties which hold simultaneously in nonrelativistic physics. Distinct mathematical objects one can introduce with the same nonrelativistic limits simply describe different aspects of the more complex relativistic landscape.

The qualitative behavior of the acceleration hyperbola for circular orbits as a function of position in the r-θ plane can be understood in terms of the geometry of the relative motion as seen by the ZAMO's[16,17] by starting with the nonrotating black hole case. In the Schwarzschild spacetime, this behavior is largely the result of the competition between the (unique) relative centripetal acceleration of the circular motion, tilted away from the equatorial plane by the spatial geometry, and the outward acceleration necessary to resist falling into the hole, scaled by a proper time dilation factor. Turning on the rotation of the hole then breaks the symmetry between corevolving and counter-revolving orbits, spreading apart the asymptotes from the symmetry axis of the degenerate acceleration half-line hyperbola branch, tilting the counter-revolving orbit half farther from the black hole symmetry axis and the corevolving half closer towards it due to an increased/decreased radial acceleration term, while moving the vertex slightly away from the equatorial plane off the $\partial_{\hat{r}}$ axis.

Since the circular orbit motion is a case of purely transverse relative acceleration, the acceleration vector already lies in the observer local rest space and so

may itself be directly represented by its relative observer decomposition (given by $a(U) = \gamma A(U,u)$ in Eq. (9.3) of reference [17] with $u = n$). Since the acceleration lies in the $\partial_{\hat{r}}$-$\partial_{\hat{\theta}}$ plane, it is convenient to introduce the orthonormal 2-vector notation $\vec{X} = (X^{\hat{r}}, X^{\hat{\theta}})$. For the ZAMO decomposition, the two nonzero acceleration components have the form

$$\begin{aligned}\vec{a} &= \vec{k}\sinh^2\alpha + 2\vec{\theta}_{\hat{\phi}}\sinh\alpha\cosh\alpha + \vec{A}\cosh^2\alpha \\ &= (\vec{k}+\vec{A})\sinh^2\alpha + 2\vec{\theta}_{\hat{\phi}}\sinh\alpha\cosh\alpha + \vec{A} \\ &= \frac{1}{2}(\vec{k}+\vec{A})\cosh 2\alpha + \vec{\theta}_{\hat{\phi}}\sinh 2\alpha + \frac{1}{2}(-\vec{k}+\vec{A}) \ . \end{aligned} \tag{20}$$

The first line is its relative observer decomposition into a relative centripetal acceleration term involving the relative Lie curvature vector $\vec{k}$ of the ϕ coordinate circles in the slicing geometry of the ZAMO's (see Eq. (13.3) of reference [16]), a gravitomagnetic term involving the observer expansion tensor $\theta^{\alpha}{}_{\beta}$ (let $\vec{\theta}_{\hat{\phi}} = (\theta^{\hat{r}}{}_{\hat{\phi}}, \theta^{\hat{\theta}}{}_{\hat{\phi}})$), and a gravitoelectric term involving the observer acceleration $\vec{A}$. The second line is the corresponding optical metric decomposition, where the first term is the relative Lie optical centripetal acceleration and $\vec{k}+\vec{A} = N^{-1}\vec{\tilde{k}}$ is along the optical Lie relative curvature vector of the ϕ-coordinate circles in the optical slicing geometry of the ZAMO's (see equation (13.4) of reference [16] and [18]) and the remaining two terms are the optical gravitomagnetic and gravitoelectric terms. The final line identifies the coefficients in the standard hyperbola parametrization in equation (17).

The ZAMO Lie Frenet-Serret frame is $\{\partial_{\hat{\phi}}, \hat{k}, \partial_{\hat{\phi}} \times_n \hat{k}\}$, where $\hat{k}$ is the unit vector direction of $\vec{k}$.[3] The ZAMO Fermi-Walker and corotating Fermi-Walker relative curvature vectors agree (zero vorticity condition) and are related to the Lie one by a speed-dependent relationship

$$\vec{k}_{(\mathrm{fw})} = \vec{k} + \vec{\theta}_{\hat{\phi}}/\tanh\alpha \ , \tag{21}$$

which absorbs half of the second term in the first line of (20) into the first.

For the static observer decomposition, the ZAMO gravitomagnetic expansion vector $\vec{\theta}_{\hat{\phi}} \sim \theta^{\alpha}{}_{\beta}\hat{\nu}^{\beta}$ term is instead replaced by the gravitomagnetic cross product $\hat{\nu} \times_m \vec{H}$, where $\vec{H} = 2\omega$ is twice the vorticity of the static observer 4-velocity m and $\hat{\nu}$ is the unit relative velocity with respect to the relevant observer. In the static observer case, the Lie and corotating Fermi-Walker relative curvature vectors agree (zero expansion condition) and are related to the Fermi-Walker relative curvature by an analogous relationship.

Each of these decompositions views the circular orbit from the point of view of an observer family also in circular motion. If instead one wishes to view this relative motion from the point of view of the circular orbit, one needs a comoving frame along that orbit, and one can perform a Frenet-Serret analysis of the derivative properties of the relative velocity vector of the test particle following the orbit with respect to either family but as seen by the test particle itself, as discussed in a companion article in these proceedings.[3] This comoving relative Frenet-Serret

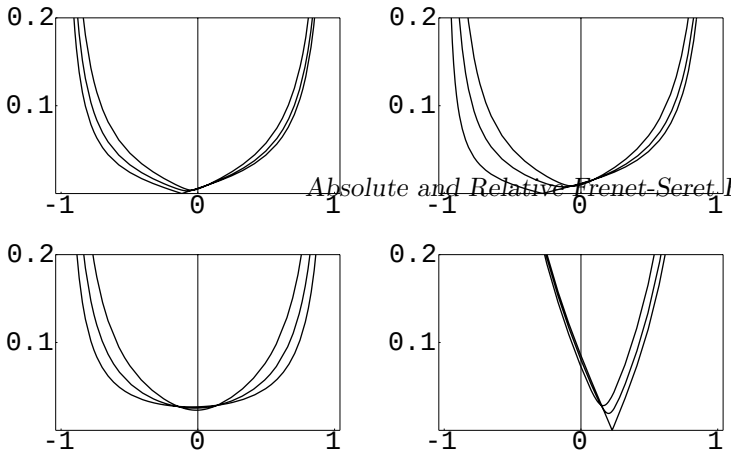

Figure 8: The magnitude $||\omega_{(\mathrm{FW})}||$ of the Fermi-Walker angular velocity versus velocity shown at angles $\theta = \pi/3$, $\pi/2.5$, $\pi/2.01$ at the same radii as in figure 3 for $\bar{a} = 0.5$: (a) $\bar{r} = 5$ (region A, upper left), (b) $\bar{r} = 4$ (region A, upper right), (c) $\bar{r} = 3$ (region B, lower left), (d) $\bar{r} = 2.25$ (region C, lower right).

frame coincides with the spatial frame of the spacetime Frenet-Serret frame.[3] Thus modulo the boosts between local rest spaces, the spacetime Frenet-Serret frame is intimately connected with the various relative Frenet-Serret frames which shape our picture of what is happening in the gravitational field of the black hole.

To describe accelerated photon circular orbits, one can choose the limits $\nu \to \pm 1$ of $\gamma^{-1}U$ and $\gamma^{-2}a$ (corresponding to a unit energy affine parameter[16]), yielding respectively the 4-momenta $P_\pm = n \pm \partial_{\hat{\phi}}$ and the corresponding acceleration vectors

$$\vec{a}_\pm = \vec{k} + \vec{A} \pm 2\vec{\theta}_{\hat{\phi}} \ , \tag{22}$$

where the $+/-$ sign refers to the corevolving/counter-revolving photon orbits. These two vectors give the directions of the asymptotes of the timelike circular orbit acceleration hyperbola, which are the the diagonals of the two parallelograms formed by the vectors $\pm\vec{\theta}_{\hat{\phi}}$ and $(\vec{k} + \vec{A})/2$ (modulo a factor of 2) thought of as tangent to the hyperbola center at $(-\vec{k} + \vec{A})/2$, as the third line of equation (20) reveals.

It is worth noting that these vectors and their average can be expressed in the form

$$\vec{a}_\pm = \mp(\tilde{g}_{\phi\phi})^{1/2}\vec{\nabla}\zeta_\pm \ , \qquad (\vec{a}_+ + \vec{a}_-)/2 = \vec{k} + \vec{A} = -\vec{\nabla}\ln(\tilde{g}_{\phi\phi})^{1/2} \tag{23}$$

where $\zeta_\pm = -N^\phi \pm (\tilde{g}_{\phi\phi})^{-1/2}$ are the photon angular velocities (see equation (33)), $\tilde{g}_{\phi\phi} = N^{-2}g_{\phi\phi}$ is the corresponding optical metric component, and $\vec{\nabla} = (\partial_{\hat{r}}, \partial_{\hat{\theta}})$. Thus their lines of force can be represented as orthogonal trajectories to these three potential functions. The surfaces associated with the last potential function are the generalizations to the rotating black hole case of the von Zeipel cylinders discussed for Schwarzschild by Abramowicz.[19] Along the lines of force of the vector field $\vec{k} + \vec{A}$ in the ρ-z coordinate plane, r decreases in region A (r component negative, points radially inward) and increases in region C (r component positive, points radially outward), with the transition between these inward and outward behaviors occurring in region B. The lines of force of the photon accelerations $\vec{a}_\pm$ are respectively more inward (+) and more outward (−) compared to this vector field whose direction lies nearly midway between the two.

By extremizing the distance between the acceleration hyperbola and its center, one easily finds its vertex rapidity $\alpha_{(\mathrm{vert})}$ to satisfy the following condition (which

can be represented equivalently in the second form)

$$\tanh 4\alpha_{(\mathrm{vert})} = -2\left(\frac{\vec{k}+\vec{A}}{2}\right)\cdot\vec{\theta}_{\hat{\phi}}/(||\frac{\vec{k}+\vec{A}}{2}||^2 + ||\vec{\theta}_{\hat{\phi}}||^2)$$
$$\alpha_{(\mathrm{vert})} = \frac{1}{4}\ln(||\vec{a}_-||/||\vec{a}_+||\ , \tag{24}$$

which also determines the vertex of the closely related Frenet-Serret angular velocity hyperbola at which $||\omega_{(\mathrm{FS})}||$ is minimized. The corresponding relative velocity $\nu_{(\mathrm{vert})} = \tanh\alpha_{(\mathrm{vert})}$ is shown in figure 4 of [8], counter-revolving until very near the horizon where it becomes corevolving.

Figure 8 shows a plot of the magnitude $||\omega_{(\mathrm{FW})}||$ of the Fermi-Walker angular velocity versus velocity for selected radii and angles. The minima occur at the vertex observer velocity $\nu_{(\mathrm{vert})}$. Approaching the equatorial plane a kink develops corresponding to the limiting minimum value of zero assumed by $||\omega_{(\mathrm{FW})}||$ at the extremely accelerated observers there in region A (counter-revolving) and in region C (corevolving), while a smooth minimum occurs in region B in the equatorial limit where the velocity makes a transition between the null limiting velocities at the AB (counter-revolving) and BC (corevolving) interfaces. The latter observers are referred to as the spin critical observers in [9], but figure 7(b) there incorrectly shows their velocity going beyond $|\nu| = 1$ rather than terminating on the circular photon geodesic points being approached in the acceleration vertex velocity curve in figure 4(c) of [8]. The gravitomagnetic effects associated with the expansion tensor due to the rotation of the black hole are only appreciable near the hole. The nonrotating Schwarzschild case offers an opportunity to examine the behavior of the remaining gravitoelectric and space curvature effects in the absence of the former effect. Turning on the rotation one can then see how things change.

Consider then the Schwarzschild case. The expansion tensor is zero and the nonzero orthonormal components of the acceleration vector are

$$\vec{a} = (\vec{k}+\vec{A})\sinh^2\alpha + \vec{A} = \frac{1}{2}(\vec{k}+\vec{A})\cosh 2\alpha + \frac{1}{2}(-\vec{k}+\vec{A})\ , \tag{25}$$

where

$$\vec{k} = -(r\sin\theta)^{-1}((1-2\mathcal{M}/r)^{1/2}\sin\theta, \cos\theta)\ ,$$
$$\vec{A} = ((1-2\mathcal{M}/r)^{-1/2}\mathcal{M}/r^2, 0)\ . \tag{26}$$

The relative normal $\vec{k}$ is tilted away from the equatorial plane compared to the horizontal inward flat spacetime relative normal $-\rho^{-1}(\sin\theta, \cos\theta)$ by the change $\rho^{-1} \to (\rho/\sqrt{1-2\mathcal{M}/r})^{-1}$ reflecting the dilation of radial arclength compared to coordinate radius near the hole. This contracts the radial component of the relative normal, tilting the normal away from its horizontal direction as shown in figure 9. As one approaches the horizon $\bar{r} = 2$, the radial component of $\vec{k}$ goes to zero and $\vec{k}$ becomes tangent to the horizon, pointing away from the equatorial plane.

The circular photon acceleration is the vector $\vec{k}+\vec{A}$ shown in figure 9 parallel to the acceleration half line. This vector has the same direction as the optical Lie

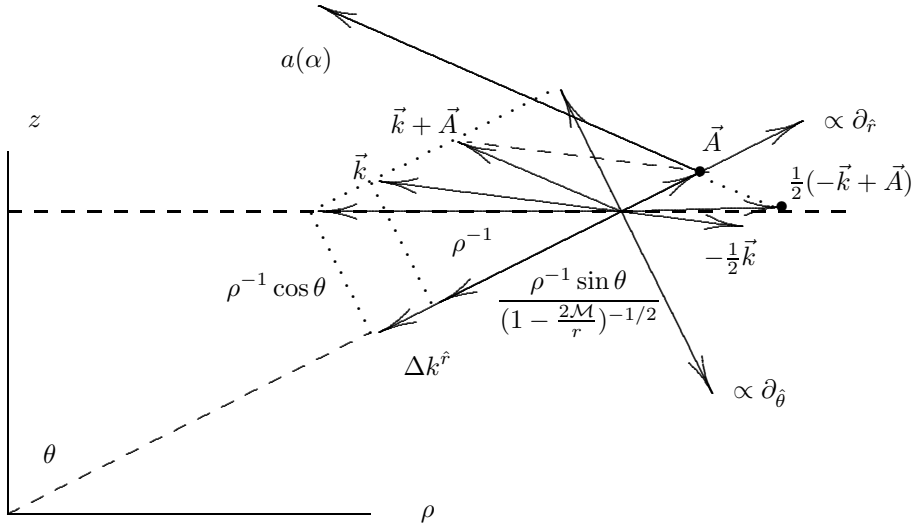

Figure 9: In the Schwarzschild case, the geometry of the ZAMO Lie relative curvature $\vec{k}$ tilted by the radial contraction $\Delta k^{\hat{r}}$, the ZAMO acceleration $\vec{A}$, the photon acceleration $\vec{k}+\vec{A}$, the timelike circular orbit degenerate acceleration hyperbola half line $a(\alpha)$ and its center at $\frac{1}{2}(-\vec{k}+\vec{A})$ in region A for the typical angle $\theta = \pi/3$, shown with the correct orientation of the acceleration plane in the ρ-z coordinate plane. The additional tilt of the half line $a(\alpha)$ above the dashed line is due to the proper time dilation factor multiplying $\vec{A}$.

curvature vector[16]

$$\tilde{\vec{k}} = N(\vec{k}+\vec{A}) = -\rho^{-1}\left(\left(1-\frac{3\mathcal{M}}{r}\right)\sin\theta, \left(1-\frac{2\mathcal{M}}{r}\right)^{1/2}\cos\theta\right) \ . \qquad (27)$$

Its radial component goes to zero at the interface $\bar{r} = 3$ between regions A and C where $\tilde{\vec{k}}$ becomes tangent to the interface circle, inside of which it the vector points radially outward rather than inward as in region A, becoming purely radial at the horizon. This is the famous "reversal of the optical centrifugal force" effect which occurs passing from region A into region C.[20]

At zero ZAMO relative velocity $\nu = 0 = \alpha$, the acceleration starts out at $\vec{A}$ on the radial axis, but the resultant of the centripetal acceleration term $\vec{k}\sinh^2\alpha$ and $\vec{A}$ scaled by the factor $\gamma^2 = 1+\sinh^2\alpha$ (reflecting the change in the proper time parametrization of the second time derivative) leads to an additional tilting of the acceleration half line (due to the term $\sinh^2\alpha$) compared to the resultant of the centripetal acceleration and $\vec{A}$ alone. Far from the hole the decrease in the radial component of $\vec{k}$

$$\Delta k^{\hat{r}} = [1-(1-2\mathcal{M}/r)^{1/2}]\rho^{-1}\sin\theta \qquad \begin{cases} \overset{r\to\infty}{\to} \frac{\mathcal{M}}{r^2}\left(1+\frac{\mathcal{M}}{2r}\right) \\ \overset{2\mathcal{M}}{\to} \frac{1}{2\mathcal{M}} \end{cases} \qquad (28)$$

is exactly compensated for by the observer acceleration

$$A^{\hat{r}} = \frac{\mathcal{M}}{r^2}\left(1-\frac{2\mathcal{M}}{r}\right)^{-1/2} \qquad \begin{cases} \overset{r\to\infty}{\to} \frac{\mathcal{M}}{r^2}\left(1+\frac{\mathcal{M}}{r}\right) \\ \overset{2\mathcal{M}}{\to} \infty \end{cases} \tag{29}$$

in the vector sum $(-\vec{k}+\vec{A})/2$ defining the center of the degenerate acceleration hyperbola, putting the center on the horizontal axis $\chi = \frac{\pi}{2} - \theta$ (see figure 9), but moving it away from the equatorial plane on the opposite side of this axis as the observer acceleration grows without bound approaching the horizon while the radial shortening factor is bounded. Both $\Delta k^{\hat{r}}$ and $A^{\hat{r}}$ are decreasing functions of r satisfying $\Delta k^{\hat{r}} < A^{\hat{r}}$.

Since $k^{\hat{r}} + A^{\hat{r}} = -r^{-1}(1-2\mathcal{M}/r)^{-1/2}(1-3\mathcal{M}/r)$ changes sign (negative in region A, positive in region C) while $A^{\hat{r}} > 0$, the component $a^{\hat{r}}$ can change sign (so that the acceleration curve crosses the $\partial_{\hat{\theta}}$-axis) only in region A. As shown in figure 6, for $\bar{r} > 3$ (region A) the degenerate acceleration hyperbola half line always intersects the $\partial_{\hat{\theta}}$-axis, but at $\bar{r} = 3$ it is parallel to this axis with a constant radial acceleration component, and for $2 < \bar{r} < 3$ (region C) this half line tilts away from the $\partial_{\hat{\theta}}$-axis, corresponding to the fact that the acceleration must always be radially outward to resist the strong attraction to the hole no matter what value the velocity has.

The acceleration is symmetric under the transformation $\nu \to -\nu$ (or $\alpha \to -\alpha$) which interchanges the corevolving and counter-revolving orbits in the Schwarzschild case. To leading order in the black hole angular momentum parameter a, the nonzero observer expansion tensor components and additional acceleration component are

$$(\theta^{\hat{r}}{}_{\hat{\phi}}, \theta^{\hat{\theta}}{}_{\hat{\phi}}) \to \frac{\mathcal{M}a}{r^3}\sin\theta(-3, \frac{a^2}{r^2}\sin 2\theta) \ , \ A^{\hat{\theta}} \to -\frac{\mathcal{M}a^2}{r^3}\sin 2\theta \ . \tag{30}$$

As one turns on the angular momentum parameter a from 0 to a small positive value, the leading order effect is the introduction of a small radially inward symmetry breaking term $-(3\mathcal{M}a/r^2)\sin\theta\sinh 2\alpha$ which separates the corevolving and counter-revolving acceleration vectors in the radial direction by equal amounts about the $\bar{a} = 0$ acceleration half line, with the counter-rotating/counter-rotating orbits experiencing an increased/decreased radial acceleration due to the gravitomagnetic field. The small nonzero component $A^{\hat{\theta}}$ shifts the vertex of the acceleration hyperbola slightly off the $\partial_{\hat{r}}$-axis, tilting $\vec{A}$ away from the equatorial plane. These effects qualitatively describe the situation for all physical values $0 < \bar{a} \leq 1$ since the vector $\vec{\theta}_{\hat{\phi}}$ is always radial to within less than about 1% at its most extreme value not far from the horizon ($|\theta^{\hat{\theta}}{}_{\hat{\phi}}/\theta^{\hat{r}}{}_{\hat{\phi}}| \lesssim .01$), while $\vec{A}$ is always radial to within less than about 5% at its most extreme value not far from the horizon. Thus the acceleration half line parallel to $(\vec{k}+\vec{A})\cosh 2\alpha$ terminating at $\vec{A}$ (combined spatial geometry and gravitoelectric terms) is split into the two halves of the one branch of the acceleration hyperbola by the addition of the nearly radial vector fields $\pm 2\vec{\theta}_{\hat{\phi}}|\sinh 2\alpha|$ (the gravitomagnetic term) which pulls the counter-rotating acceleration farther away from the symmetry axis $\rho = 0$.

7 Concluding remarks

The Frenet-Serret properties of circular orbits analyzed from the point of view of the ZAMOs help bridge the gap between the Newtonian and general relativistic pictures of the gravitational field of a central source. The past decade has seen a large number of articles written about circular orbits and their interpretation in terms of space-plus-time concepts, but the situation has remained somewhat cloudy. By combining the relative observer machinery with the Frenet-Serret approach in various ways, one begins to see how our nonrelativistic ideas stretch to fit into the relativistic setting and how they relate to the Fermat's principle (conformal) approach.

References

1. Bini D, Carini P and Jantzen R T 1999 *Proceedings of the Eighth Marcel Grossmann Meeting on General Relativity (1997)* ed T Piran (Singapore: World Scientific)
2. Bini D, de Felice F and Jantzen R T 1999 *Proceedings of the Third William Fairbank Meeting on the Lense-Thirring Effect (1998)* ed C Sigismondi (Singapore: World Scientific)
3. Bini D, de Felice F and Jantzen R T 1999 *Class. Quantum Grav.* **16** 2105
4. Iyer B R and Vishveshwara C V 1993 *Phys. Rev.* **D48** 5706
5. Hönig E, Schücking E L and Vishveshwara C W 1974 *J. Math. Phys.* **15** 744
6. Synge J L 1960 *Relativity: The General Theory* (Amsterdam: North Holland)
7. Wilkins D 1972 *Phys. Rev.* **5** 814
8. Bini D, Jantzen R T and Merloni A 1999 *Class. Quantum Grav.* **16** 1333
9. Bini D, Carini P and Jantzen R T 1997 *Int. J. Mod. Phys.* **D6** 143
10. Page D 1998 *Class. Quant. Grav.* **15** 1669
11. Semerák O 1996 *Gen. Relativ. Grav.* **28** 1151
12. Semerák O 1998 *Gen. Relativ. Grav.* **30** 1203
13. Semerák O 1994 *Astron. Astrophys.* **291** 679
14. Bini D, Carini P and Jantzen R T 1992 *Proceedings of the Third Italian-Korean Astrophysics Meeting* ed S. Kim, H. Lee and K.T. Kim *J. Korean Phys. Soc.* **25** S190
15. de Felice F 1995 *Class. Quantum Grav.* **12** 1119; de Felice F and Usseglio-Tomasset S 1991 *Class. Quantum Grav.* **8**, 1871
16. Bini D, Carini P and Jantzen R T 1997 *Int. J. Mod. Phys.* **D6** 1
17. Jantzen R T, Carini P and Bini D 1992 *Ann. Phys. (N.Y.)* **215** 1
18. Abramowicz M A, Nurowski P Wex N 1995 *Class. Quantum Grav.* **12** 1467
19. Abramowicz M A 1990 *Mon. Not. R. Ast. Soc.* **245** 733
20. Abramowicz M A and Prasanna A R 1990 *Mon. Not. R. Ast. Soc.* **245** 720
21. Misner C W, Thorne K S and Wheeler J A 1973 *Gravitation* (San Francisco: Freeman)

Appendix: The Kerr computational quantities

To study the geometry of the acceleration and Frenet-Serret angular velocity hyperbolae in the Kerr spacetime, one needs the ZAMO computational quantities for the Kerr metric.[21] With some convenient abbreviations associated with the Boyer-Lindquist coordinate system, including formulas for the radius of the horizon ($N = 0$) and ergosphere, and the angular velocities

$$\zeta_\pm = -N^\phi \pm N(g_{\phi\phi})^{-1/2} \tag{31}$$

of the circular photon orbits, which follow from the general angular-physical velocity component relations

$$\zeta = -N^\phi + N(g_{\phi\phi})^{-1/2}\nu^{\hat{\phi}}_{(n)} \tag{32}$$

obtained by solving for the roots of the expression (2.3) of [9] for the coordinate gamma factor of U, one needs the lapse, shift, and spatial metric coordinate components for the ZAMO observers, the ZAMO Lie curvature vector components, and the ZAMO kinematical quantities, namely the nonzero components of the acceleration vector A^α (minus the gravitoelectric field g) and expansion tensor $\theta^\alpha{}_\beta$ (minus half the Lie gravitomagnetic tensor field $H^\alpha{}_\beta$[16]). The optical Lie curvature vector components $\tilde{\vec{k}} = N(\vec{k}+\vec{A})$ are also given, together with the angular velocity variable roots of the acceleration components $a^{\hat{r}}$ and $a^{\hat{\theta}}$. Finally the curves separating the regions A, B, and C in the ρ-z coordinate plane are derived.

Convenient abbreviations and formulas

$$\begin{aligned}
&(c, s) = (\cos\theta, \sin\theta)\\
&\rho^2 = r^2 + a^2c^2\ ,\ \epsilon = r^2 - a^2s^2\\
&\Delta = r^2 + a^2 - 2\mathcal{M}r\\
&\Lambda = (r^2 + a^2)\rho^2 + 2\mathcal{M}ra^2s^2\\
&r_{(\mathrm{erg})} = \mathcal{M} + \sqrt{\mathcal{M}^2 - a^2c^2}\\
&r_{(\mathrm{h})} = \mathcal{M} + \sqrt{\mathcal{M}^2 - a^2}\\
&\zeta_\pm = \frac{2a\mathcal{M}rs \pm \rho^2\sqrt{\Delta}}{\Lambda s} = \frac{\rho^2 - 2\mathcal{M}r}{s(-2a\mathcal{M}rs \pm \rho^2\sqrt{\Delta})}
\end{aligned} \tag{33}$$

Metric (ZAMO decomposition)

$$\begin{aligned}
&(N, N^\phi) = \left(\sqrt{\frac{\Delta\rho^2}{\Lambda}}, -\frac{2a\mathcal{M}r}{\Lambda}\right)\\
&(g_{rr}, g_{\theta\theta}, g_{\phi\phi}, \sqrt{g}) = \left(\frac{\rho^2}{\Delta}, \rho^2, \frac{\Lambda s^2}{\rho^2}, \frac{\rho^2 s}{N}\right)
\end{aligned} \tag{34}$$

ZAMO relative curvature vector and optical counterpart

$$
\begin{aligned}
(k^{\hat{r}}, k^{\hat{\theta}}) &= \left(-\frac{\sqrt{\Delta}}{\rho^3\Lambda}[r\rho^4 - \mathcal{M}a^2s^2\epsilon], -\frac{c}{\rho^3 s\Lambda}[\Lambda(r^2+a^2) - \Delta a^2 s^2\rho^2] \right) \\
\tilde{k}^{\hat{r}} &= \frac{1}{\rho^2\Lambda^{3/2}}\left[m\rho^2(r^4-a^4) + \Delta[ma^2s^2(3r^2-a^2c^2) - r\rho^4]\right] \\
\tilde{k}^{\hat{\theta}} &= -\frac{\sqrt{\Delta}}{\rho^2\Lambda^{3/2}}\left[\rho^2\Lambda\cot\theta + 4a^2mrsc(r^2+a^2)\right]
\end{aligned}
\tag{35}
$$

ZAMO kinematical quantities

$$
(A^{\hat{r}}, A^{\hat{\theta}}) = \left(\frac{\mathcal{M}}{\rho^3\Lambda\sqrt{\Delta}}[\rho^2(r^4-a^4) + 2\Delta r^2a^2s^2], -\frac{2a^2\mathcal{M}r}{\rho^3\Lambda}(r^2+a^2)sc \right) \tag{36}
$$

$$
(\theta^{\hat{r}}{}_{\hat{\phi}}, \theta^{\hat{\theta}}{}_{\hat{\phi}}) = \left(\frac{a\mathcal{M}}{\Lambda\rho^3}[(r^2+a^2)(a^2-3r^2) - a^2s^2(a^2-r^2)]s, \frac{2a^3\mathcal{M}r\sqrt{\Delta}}{\Lambda\rho^3}s^2c \right)
$$

Roots of acceleration components (angular velocity)

$$
\zeta_\pm^{(r)} = s^{-1}[as \mp \rho^2\sqrt{r/(\mathcal{M}\epsilon)}]^{-1} \tag{37}
$$

$$
\zeta_\pm^{(\theta)} = \frac{2\mathcal{M}ra(r^2+a^2 \pm ia\rho^2\sqrt{2\mathcal{M}r\Delta})}{(r^2+a^2)^3 - \Delta a^2s^2(r^2+a^2+\rho^2)} \tag{38}
$$

The regions A, B and C

Timelike circular orbits with vanishing radial acceleration have 4-velocity $U_\pm^{(r)} = \Gamma_\pm^{(r)}(\partial_t + \zeta_\pm^{(r)}\partial_\phi)$ and coordinate angular velocity $\zeta_\pm^{(r)}$ given above. They become null (i.e., coincide with photon orbits) at the interface radii $r_{AB}(\theta)$ (counter-rotating photon: $-$) and $r_{BC}(\theta)$ (corotating photon: $+$) characterized by the condition $\zeta_\pm^{(r)} = \zeta_\pm$. A straightforward calculation shows that this relation is equivalent to

$$
\sqrt{\Delta} \mp as = \sqrt{\mathcal{M}\epsilon/r}, \tag{39}
$$

or

$$
a^2s^2(r-\mathcal{M}) \mp 2ars\sqrt{\Delta} + [\Delta r - \mathcal{M}(r^2-a^2)] = 0\ , \tag{40}
$$

which are implicit equations for r as a function of θ that are quadratic in s and so easily solved for θ as a function of r for the two curves $\theta = \theta_{\rm AB}(r)$ and $\theta = \theta_{\rm BC}(r)$

$$
\begin{aligned}
\theta_{\rm AB}(r) &= \arcsin S\ ,\ 0 \le S \le 1\ , \\
\theta_{\rm BC}(r) &= \arcsin S\ ,\ -1 \le S \le 0\ , \\
S &= \frac{r\sqrt{\Delta} - \sqrt{m}\sqrt{2r^3 - 3mr^2 + ma^2}}{a(r-m)}\ .
\end{aligned}
\tag{41}
$$

Figures 4(a),(b),(c) are plots of these curves for the cases $\bar{a} = 0, 0.5, 1$ respectively.

In the extreme case $\bar{a} = 1$, equation (40) can be factored into the form

$$(r - \mathcal{M})[s^2 \pm 2rs + (r^2 - \mathcal{M}^2 - 2\mathcal{M}r)] = 0 \tag{42}$$

which exhibits a bifurcating behaviour at the horizon for the curve $r = r_{\rm BC}(\theta)$. The $r = r_{\rm BC}(\theta)$ solution of (42) consists of two branches: a) $r = r_{\rm BC1}(\theta) = \mathcal{M} = r_{\rm (h)}$, namely the horizon itself, and b) $r = r_{\rm BC2}(\theta)$, the solution of the quadratic equation (in either r or in s) $s^2 \pm 2rs + (r^2 - \mathcal{M}^2 - 2\mathcal{M}r) = 0$. The limiting angle at which $r = r_{\rm BC2}(\theta)$ intersects the horizon is $\theta_* = \arcsin(\sqrt{3} - 1) \approx 47.1°$. This angle coincides with the maximum angle for which the stationary observers with the same fixed angular velocity as the hole $\zeta_{\rm (h))} = a^2/(a^2 + r_+^2) = 1/2$ are timelike near the horizon, and with the minimum angle of the single corotating horizon skimming[7] photon spherical geodesic orbit at the horizon. The latter follows by expressing the coefficients of equation (29) of[7] for $z = \cos^2\theta$ entirely in terms of the energy constant E using equation (22), leading to $E^2 = (z^2 - 1)/(z^2 + 6z - 3)$; the limit $E \to \infty$ for a photon corresponds to $z = 2\sqrt{3} - 3$, equivalent to $\theta = \theta_*$.